Journal of Power Sources 189 (2009) 828–831

Contents lists available at ScienceDirect

Journal of Power Sources

journal homepage: www.elsevier.com/locate/jpowsour

Short communication

Synthesis and performance of Zn_2SnO_4 as anode materials for lithium ion batteries by hydrothermal method

X.J. Zhu[a,*], L.M. Geng[a], F.Q. Zhang[b], Y.X. Liu[a], L.B. Cheng[a]

[a] College of Chemistry, Central China Normal University, Wuhan, Hubei 430079, China
[b] Library, Central China Normal University, Wuhan, Hubei 430079, China

ARTICLE INFO

Article history:
Received 16 June 2008
Received in revised form 13 July 2008
Accepted 16 July 2008
Available online 23 July 2008

Keywords:
Hydrothermal method
Zinc stannate
Lithium ion batteries
Anode materials

ABSTRACT

Inverse spinel structure Zn_2SnO_4 was successfully synthesized by a simple hydrothermal process using NaOH as an alkaline mineralizer. The hydrothermal conditions, such as alkaline concentration and synthesis temperature, have an important influence on the structure and performance of the product. The structural, morphological and electrochemical properties were investigated by means of X-ray diffraction (XRD), scanning electron microscopy (SEM) and electrochemical measurement. The electrochemical test showed that Zn_2SnO_4, which was prepared at 0.2 M NaOH concentration at 220 °C for 24 h, showed 1903.6 mAh/g of initial discharge capacity and 1045.5 mAh/g of initial charge capacity. A specific discharge capacity of 644.7 mAh/g remained after 20 cycles.

1. Introduction

Various tin oxides and composite oxides have been considered as the most promising negative-electrode materials for lithium ion batteries because of their low lithium insertion potentials, high volumetric and gravimetric capacities [1,2]. However, the poor capacity retention of these new materials during cycling as well as the large irreversible capacity during the first discharge/charge cycle has limited their use in practical cells. On the other hand, zinc oxides (ZnO), which can present a high capacity of 1277–766 mAh/g in the potential range of 0.05–2.50 V vs Li^+/Li, are promising negative-electrode materials for lithium ion batteries [3].

Recently, as the composite oxide of zinc and tin, Zn_2SnO_4 attracts researchers' more attention since it has an inverse spinel structure. Zn_2SnO_4 is a very important material in advanced technologies, such as gas sensor, photoelectrochemical cells [4] and synergistic flame retardants [5]. To the best of our knowledge, little attention has been paid to Zn_2SnO_4 as anode materials for lithium ion batteries [6]. Further studies are necessary to put the new materials into practice.

In recent years, Zn_2SnO_4 has been prepared by high-temperature calcination [7–10], thermal evaporation [11], sol–gel method [12], etc. Compared with the above processes, the hydrothermal method has sparked much interest due to operational simplicity, cost-efficiency and the capability for large-scale production. Wu and co-workers [13] reported hydrothermal synthesis of ZTO crystals. In this paper Zn_2SnO_4 was synthesized by one-step hydrothermal method. It can be seen that alkaline concentration and synthesis temperature are important factors in size, crystalline and purity of final products.

2. Experimental details

All reagents were of analytical grade without further purification. In a typical experiment, $ZnSO_4{\cdot}7H_2O$ (Shanghai Hengxin Chemical Reagent Co. Ltd.) and $SnCl_4{\cdot}5H_2O$ (Shanghai Hengxin Chemical Reagent Co. Ltd.) with the molar ratio of Zn:Sn = 2:1 were used as the starting materials. They were dissolved into distilled water to form two transparent solutions, respectively. After $ZnSO_4$ solution was mixed with $SnCl_4$ solution completely, NaOH (Shanghai Hengxin Chemical Reagent Co. Ltd.) solution was added dropwise into the mixture under magnetic stirring to form white slurry. In reaction system, the feasible NaOH concentration in the mixture for the expecting product is in the range of 0.05–0.3 M. The final white slurry was transferred into Teflon-lined autoclave up to 80% of the total volume and reacted further at different hydrothermal conditions. After the reaction was terminated, the precipitate was filtered, washed with distilled water to remove Cl^- and SO_4^{2-} ions, and then dried at 80 °C for 12 h in vacuum.

* Corresponding author. Tel.: +86 27 62178945.
E-mail address: xianjunzhu@yahoo.com.cn (X.J. Zhu).

0378-7753/$ – see front matter © 2008 Elsevier B.V. All rights reserved.
doi:10.1016/j.jpowsour.2008.07.028

The completion of the reaction and the phase purity of the samples were confirmed by X-ray diffraction (XRD, Rigaku D/max-2500).

The morphology and particle size of the samples was observed with field emission scanning electron microscope (JEOL, JSM-6700F).

The discharge/charge tests were performed using CR2016 coin-type cell by an automatic battery tester system (Land®, China). Coin-type test cells were assembled in an argon glove box using a Celgard 2400 as a separator, 1 M $LiClO_4$ in ethylene carbonate (EC)/diethyl carbonate (DMC) (1:1 volume ratio) as an electrolyte (Zhangjiagang, China), and Li foil as counter and reference electrodes. The working electrode was prepared by pressing a mixture of the active materials, acetylene black and PTFE in weight ratio of 4:4:2. Discharge/charge measurements were performed in the voltage range of 0.05–3.00 V at the current density of 50 mA/g. Cyclic voltammograms were measured by three electrode system using CHI650A electrochemical analyzer (Shanghai, China) at a scan rate of 0.05 mV/s. Li was as counter and reference electrodes, and 1 M $LiClO_4$ in ethylene carbonate (EC)/diethyl carbonate (DMC) (1:1 volume ratio) as an electrolyte.

3. Results and discussion

Fig. 1 shows the XRD patterns of the as-prepared samples at different alkaline concentration in the hydrothermal temperature of 220 °C for 24 h. As shown in Fig. 1, all main diffraction peaks of the four samples are consistent with the JCPDS (24-1470) data of the pure reverse-spinel Zn_2SnO_4. When NaOH concentrations are 0.05 and 0.10 M, there are impurity peaks, which are identified as SnO_2. With an increase of NaOH concentration as showed from Fig. 1a–c, peaks attributed to Zn_2SnO_4 in the XRD patterns became stronger. At a concentration of 0.2 M NaOH, pure Zn_2SnO_4 is formed because no impurity phases were detected. These results can be described as follow:

$$2ZnSO_4 + SnCl_4 + 8NaOH \leftrightharpoons Zn_2SnO_4 + 2Na_2SO_4 + 4NaCl + 4H_2O \quad (1)$$

Further increasing NaOH concentration to 0.3 M (Fig. 1d), ZnO as a co-product appeared. The reason may be due to thermodynamical nucleation and stability as well as dynamical growth, resulting that the hydrothermal reaction should be carried out at an optimum concentration of NaOH to promote Zn_2SnO_4 crystallization. In the present study, the optimum NaOH concentration is 0.2 M. It demonstrated that the NaOH concentration is a critical factor influencing the crystallinity, morphology and size of the as-prepared samples. It can also prove that the hydrothermal temperature is another key factor in the present study. Fig. 2 is XRD patterns of the as-prepared products at various hydrothermal temperatures in 0.2 M NaOH concentration. As seen from Fig. 2, when the hydrothermal temperatures were 200 and 240 °C, there were both ZnO and SnO_2 in the final products. This is because at lower hydrothermal temperature (200 °C), ZnO and SnO_2 were generated resulting from no energy enough to promote Zn_2SnO_4 formation; On the other hand, at higher hydrothermal temperature (240 °C), Zn_2SnO_4 may partly decompose to produce ZnO and SnO_2; At the optimum temperature of 220 °C, Zn_2SnO_4 can be completely formed, and no ZnO or SnO_2 existed in the product. In order to obtain pure and better Zn_2SnO_4 crystallinity, the NaOH concentration is 0.2 M and the hydrothermal temperature is 220 °C at Zn:Sn = 2:1. By Rietveld refinement on the XRD pattern of Zn_2SnO_4 synthesized at 220 °C in 0.2 M NaOH, the lattice parameters is 8.664(3) Å.

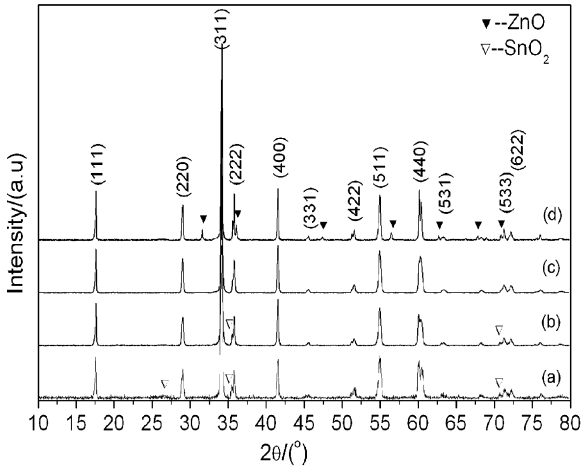

Fig. 1. XRD patterns of Zn_2SnO_4 synthesized in 220 °C for 24 h at different NaOH concentrations: (a) 0.05 M, (b) 0.1 M, (c) 0.2 M and (d) 0.3 M.

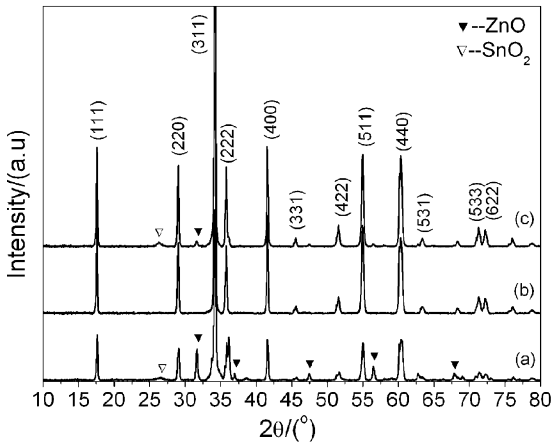

Fig. 2. XRD patterns of Zn_2SnO_4 synthesized in 0.2 M NaOH for 24 h at different hydrothermal temperatures: (a) 200 °C, (b) 220 °C and (c) 240 °C.

The SEM photograph of the samples prepared at different NaOH concentrations at 220 °C for 24 h is given in Fig. 3. As seen from the photograph, when NaOH concentration is 0.1 M, the as-prepared sample is of homogeneous distribution with a particle size 1.0 μm. When NaOH concentration is 0.2 M, the particle becomes larger, about 1.5 μm with clearly regular cubic shape. With NaOH concentration increased to 0.3 M, its morphology is different. For 0.3 M-sample, besides cube-shaped Zn_2SnO_4, there are rod-shaped and irregular-shaped impurities, which is identified as ZnO and SnO_2 by XRD. Moreover, the particle has a large distribution in grain size. The SEM photograph shows that the alkaline concentration is an important parameter influencing the size, morphology and purity of Zn_2SnO_4 particle.

Fig. 4 shows the initial three discharge/charge curves of the samples prepared in different NaOH concentrations at the current density of 50 mA/g between 0.05 and 3.0 V. It can be seen that the initial discharge/charge capacities are 1844.7/783.3, 1903.6/1045.5 and 2157.0/963.7 mAh/g for 0.1 M-, 0.2 M- and 0.3 M-sample, respectively, indicating that the initial discharge specific capacity increases with the increase of NaOH concentration, and its initial charge specific capacity increases first and then decreases with NaOH concentration increase. The 0.2 M-sample has the highest initial charge capacity (1045.5 mAh/g), and its initial discharge/charge capacity loss is the smallest (858.1 mAh/g). For the initial discharge/charge curves of 0.1 M- and 0.2 M-samples, there is a wide steady discharging plateau around 0.6 V, corresponding to lithium

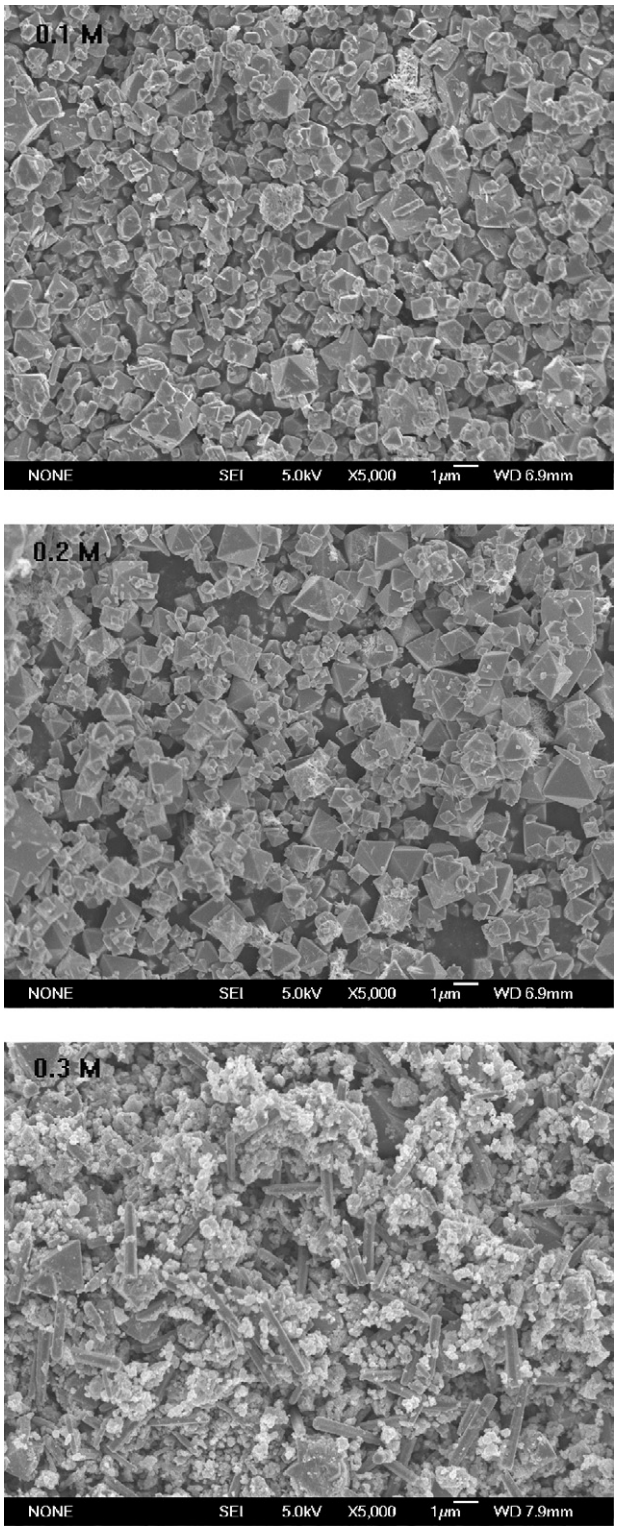

Fig. 3. SEM images of Zn_2SnO_4 samples synthesized by the hydrothermal method at 220 °C in different NaOH concentrations: (a) 0.1 M, (b) 0.2 M and (c) 0.3 M.

insertion of Zn_2SnO_4 particles and subsequently to form metallic Sn and Zn as well as Li–Sn and Li–Zn alloys. The discharge plateau of 0.2 M-sample is wider than 0.1 M-sample, exhibiting that 0.2 M-sample has larger discharge capacity. However, the discharge curve of 0.3 M-sample has no clear potential plateau around 0.6 V, and displays more inclined shape, indicating that its discharge process

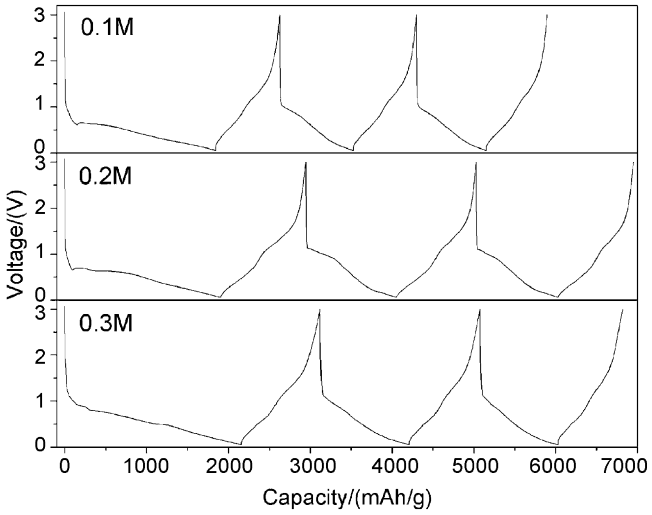

Fig. 4. The first three discharge/charge curves of Zn_2SnO_4 samples synthesized at different NaOH concentrations: (a) 0.1 M, (b) 0.2 M and (c) 0.3 M.

has any difference with that of 0.1 M- or 0.2 M-sample. From the second cycle afterward, all the potential plateaus shift upward to near 0.9 V and display more inclined shape (Fig. 5).

Cyclic voltammograms of Zn_2SnO_4 prepared at 220 °C and in 0.2 M NaOH are shown in Fig. 6. It can be seen from Fig. 6a, at the first cycle the two cathodic peaks are observed at 0.41 and 0.14 V vs Li^+/Li in the voltage range of 0.05–3.00 V, corresponding to the multi-step electrochemical lithium reaction process and the wide steady discharging plateau in the first discharge curve. Meanwhile, two main anodic peaks are located near 1.34 V and 0.60 V vs Li^+/Li, corresponding to the delithiation process. In the second cycle, the cathodic peaks appear at around 0.85 V and further negative value, respectively, and the individual peak intensity and integral area also decreases, resulting from reversible capacity losses by Li_2O formation. In the following cycles, there is no substantial change in the peak potentials and curve shape, which remain similar to those in the second cycle. If the experimented voltage range of cyclic voltammogram was limited between 0.38 and 3.00 V, one cathodic peak at 0.41 V in the negative direction and one anodic peak at 1.34 V in the positive direction are observed as shown in Fig. 6b.

On the basis of the lithium storage mechanism of ZnO [3] and SnO_2 [14], the mechanism of Zn_2SnO_4 particles during dis-

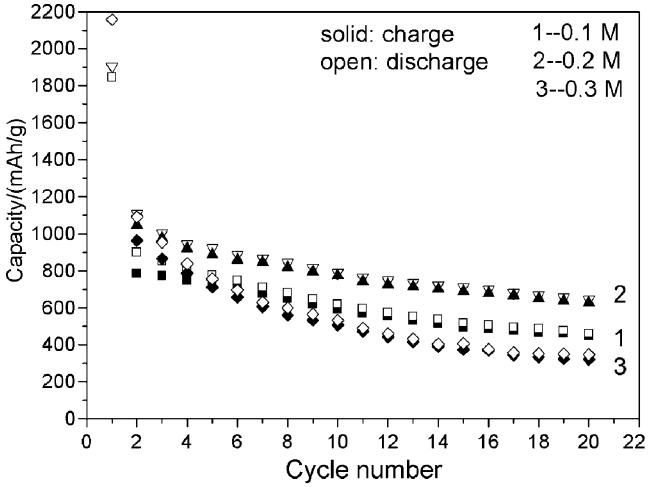

Fig. 5. Cyclability of Zn_2SnO_4 samples synthesized at different NaOH concentrations: (1) 0.1 M, (2) 0.2 M and (3) 0.3 M.

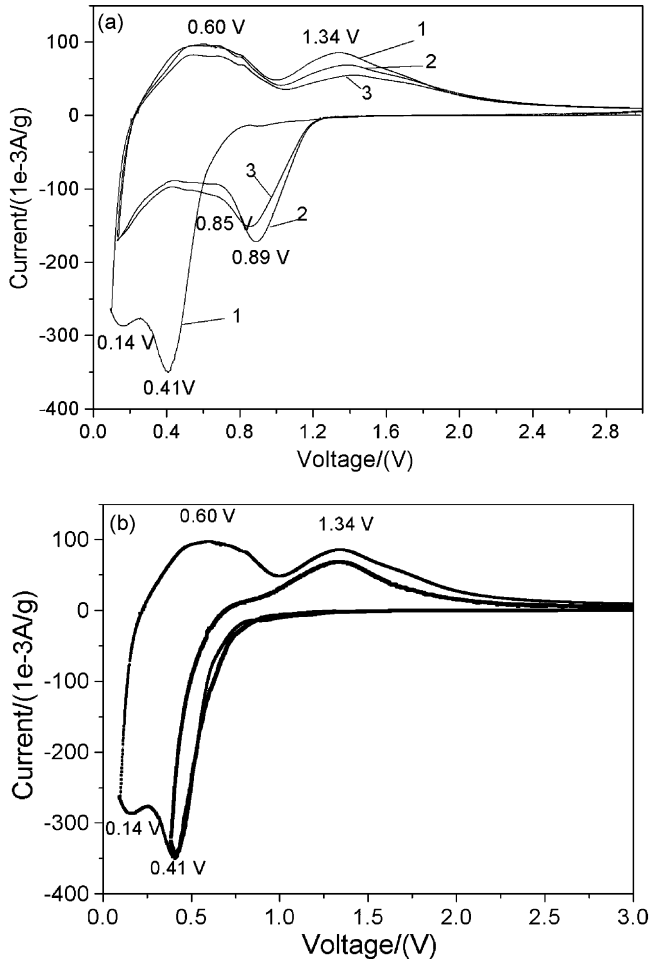

Fig. 6. Cyclic voltammograms of Zn_2SnO_4 samples synthesized in 0.2 M NaOH at a scan rate of 0.05 mV/s at different voltage ranges: (a) 0.05–3.00 V and (b) 0.38–3.00 V.

charge/charge process is as follows:

$$4Li^+ + Zn_2SnO_4 + 4e \leftrightharpoons Sn + 2Li_2O + 2ZnO \quad (2)$$

$$8Li^+ + Zn_2SnO_4 + 8e \leftrightharpoons 2Zn + Sn + 4Li_2O \quad (3)$$

$$xLi^+ + Sn + xe^- \leftrightharpoons Li_xSn \quad (0 \le x \le 4.4) \quad (4)$$

$$yLi^+ + Zn + ye^- \leftrightharpoons Li_yZn \quad (y \le 1) \quad (5)$$

The peaks of first cycle around 0.41 and 0.14 V in Fig. 6a and b correspond to the formation of Li_2O and subsequent metallic Sn or Zn as well as Li–Sn and Li–Zn alloys. After the first cycle, the peak of 0.41 V is disappeared, and is replaced by the peak of 0.89 V. The redox couple at 0.85/1.34 V is attributed to the partly reversible reactions in Eqs. (2) and (3). Another redox couple at 0.14/0.60 V is related to the formation and deformation of the Li_xSn and Li_yZn alloy in Eqs. (4) and (5). When Li_xSn and Li_yZn alloy formed, this alloying–dealloying process is reversible to some extent.

4. Conclusions

Inversed spinel Zn_2SnO_4 was synthesized by hydrothermal method. Alkaline concentrations and synthesizing temperatures are the key factors determining particle size, morphology, and purity of the product. When NaOH concentration is 0.2 M and the hydrothermal synthesizing temperature is 220 °C, the resulting product is characteristic of pure Zn_2SnO_4 phase. Electrochemical test shows that Zn_2SnO_4 synthesized at 220 °C in 0.2 M NaOH has 1903.6 mAh/g of the initial discharge capacity and 1045.5 mAh/g of the first charge capacity. It has relatively good capacity retention. However, the electrode cycle life still needs to be further improved for practical application.

Acknowledgements

This research was sponsored by the Natural Science Foundation of Hubei Province (No. 2006ABA317). The authors would like to thank Prof. H.X. Liu for his guide at Wuhan University of Technology. We also thank Prof. Y.H. Zhou for his guide and help at Wuhan University.

References

[1] S. Machill, T. Shodai, Y. Sakurai, J. Yamaki, J. Power Sources 73 (1998) 216.
[2] J.Y. Lee, R.F. Zhang, Z.L. Liu, J. Power Sources 90 (2000) 70.
[3] Z.F. Zheng, X.P. Gao, G.L. Pan, J.L. Bao, J.Q. Qu, F. Wu, D.Y. Song, Chin. J. Inorg. Chem. 20 (2004) 488.
[4] B. Tan, E. Toman, Y.G. Li, Y.Y. Wu, JACS 129 (2007) 4162.
[5] A. Petsom, S. Roengsumran, A. Ariyaphattanakul, P. Sangvanich, Polym. Degrad. Stabil. 80 (2003) 17.
[6] A. Rong, X.P. Gao, G.R. Li, T.Y. Yan, H.Y. Zhu, J.Q. Qu, D.Y. Song, J. Phys. Chem. B 110 (2006) 14754.
[7] J.X. Wang, S.S. Xie, H.J. Yuan, X.Q. Yan, D.F. Liu, Y. Gao, Z.P. Zhou, L. Song, L.F. Liu, X.W. Zhao, X.Y. Dou, W.Y. Zhou, G. Wang, Solid State Commun. 131 (2004) 435.
[8] Y. Li, X.L. Ma, Phys. Status Sol. A 202 (2005) 435.
[9] Z.G. Lu, Y.G. Tang, Mater. Chem. Phys. 92 (2005) 5.
[10] I. Stambolova, A. Toneva, V. Blaskov, D. Radev, Y. Tsvetanova, S. Vassilev, P. Peshev, J. Alloys Compd. 391 (2005) L1.
[11] J.X. Wang, S.S. Xie, Y. Gao, X.Q. Yan, D.F. Liu, H.J. Yuan, Z.P. Zhou, L. Song, L.F. Liu, W.Y. Zhou, G. Wang, J. Cryst. Growth 267 (2004) 177.
[12] G. Fu, H. Chen, Z.X. Chen, J.X. Zhang, H. Kohler, Sens. Actuators B 81 (2002) 308.
[13] J. Fang, A.H. Huang, P.X. Zhu, N.S. Xu, J.Q. Xie, J.S. Chi, S.H. Feng, R.R. Xu, M.M. Wu, Mater. Res. Bull. 36 (2001) 1391.
[14] F. Belliard, P.A. Connor, J.T.S. Irvine, Solid State Ionics 135 (2000) 163.